Swarm of Magnetic Nanoparticles Steering in Multi-Bifurcation Vessels under Fluid Flow

Ali Kafash Hoshiar[1*], Tuan-Anh Le[2], Pietro Valdastri[3], Jungwon Yoon[2*]

[1] School of Computer Science and Electronic Engineering, University of Essex, Colchester, CO4 3SQ, UK, A.kafashhoshiar@essex.ac.uk

[2] School of Integrated Technology, Gwangju Institute of Science and Technology, 123 Cheomdangwagi-ro, Buk-gu, Gwangju, Republic of Korea, 61005, jyoon@gist.ac.kr

[3] Storm Lab UK, School of Electronic and Electrical Engineering, University of Leeds, LS29JT, Leeds, UK

Abstract

Magnetic drug targeting has emerged as a promising approach for enhancing the efficiency of drug delivery. Recent developments in real-time monitoring techniques have enabled the guidance of magnetic nanoparticles (MNPs) in the vascular network. Despite recent developments in magnetic navigation, no comprehensive strategy for swarm of nanoparticles steering under fluid flow exists. This paper introduces a strategy for MNPs steering in a vascular network under fluid flow. In the proposed scheme, the swarm of nanoparticles are initially guided to an area that guarantees their successful guidance towards a desired direction (called safe zone) using an asymmetrical field function to handle swarm of nanoparticles. Then, a transporter field function is used to transfer the particles between the safe zones, and finally a sustainer field function is used to keep the particles within the safe zone. A steering algorithm is proposed to enhance the targeting performance in the multi-bifurcation vessel. Utilizing the proposed concept, a high success rate for targeting is achieved in simulations, which demonstrates the potential and limitations of swarm of nanoparticles steering under fluid flow.

Keywords:

Swarm, Magnetic nanoparticles, Electromagnetic actuation, Blood vessels, Targeted Drug Delivery

1 Introduction

In recent years many small-scale devices have emerged for mechanical interventions and biological studies [1-3]. Magnetic manipulation systems have been developed as an efficient, minimally invasive approach for medical interventions [4]. Targeted drug delivery (TDD) has emerged as one of the high potential applications of magnetic manipulation. The primary goal of TDD is to deliver drugs to the target position. Magnetic actuation-based systems have been developed to elevate the drug uptake. The principle of magnetic drug targeting (MDT) [5] is to attach the drug to the magnetic nanoparticles (MNPs) and use an external magnetic field to guide the therapeutic agent to the desired location [6, 7].

Multi-coil magnetic systems have been introduced as a solution for precise magnetic steering [8-10]. More recently, the swarm of particle based microrobots are steered under static flow conditions [11, 12]. Despite interesting results, the lack of real-time in-vivo monitoring and studies under static flow pose limitations to their medical applications.

Magnetic resonance imaging (MRI)-based navigation systems have been developed for particle steering and monitoring [13, 14]. More recently, magnetic particle imaging (MPI) based navigation systems with fast monitoring ($t<=0.5s$) and actuation were developed [15]. Considering the development of navigation systems, the strategies for MNPs steering under fluid flow are studied.

Functionalized field using electromagnetic actuator (EMA) was used to steer MNPs, prevent the MNPs from sticking and aggregating inside the vessels [16-18]. To further study the performance of drug uptake, *in-vivo* studies under functionalized magnetic field were performed in mice and their brain tissues were examined. In the absence of a magnetic force, no nanoparticles were found inside the brain. With the functionalized magnetic field, the rates of blood brain barrier (BBB) crossing and drug uptake were improved significantly [19]. Aggregation increases the force exerted on the MNPs and elevates the performance of steering of MNPs in the fluid environment. However, in real medical applications aggregation hinders the successful delivery of nanoparticles especially when pathing through anatomical barriers (e.g. BBB) is involved [20]. Moreover, gravity plays a major role in microbids (200 μm) steering [21, 22], but for much smaller sized 0.75 to 1 μm magnetic particles, the aggregation size was controlled by introducing discontinuity in the magnetic field. Thus, reducing the severity of the gravitational effects [20].

In realistic scenarios, as introduced in [23], modulated flow control (MFC) and successive targeted embolization (STE) methods can be applied to reduce and control the blood flow, which makes the proposed scheme applicable. More recent works also cover in vitro and in vivo studies using MRI based navigation systems

[21, 22]. Despite the recent developments, no electromagnetic steering strategy for swarm of nanoparticles under fluid flow have been studied. This paper introduces an electromagnetic actuation scheme for swarm of nanoparticle steering in multi-bifurcation blood vessels under magnetic force in fluid flow condition.

In the electromagnetic steering scheme, the swarms of MNPs move in the same direction as the blood flow and EMAs are used to adjust their positions. The proposed scheme considers a realistic vessel and converts it into a multi-bifurcation channel with one input and four outputs, which resembles a blood vessel (Fig. 1). It is assumed that the designed EMA can keep the rod-shaped aggregated MNPs inside a safe zone [17] (the space between the vessel boundary and the middle vessel line, as shown in Fig. 2 B) and guide them towards the desired outlet. The steering function (SF), which consists of three parts (shown in Fig. 2 C), is designed to guide the particles toward the desired outlet in the multi-bifurcation network. The main concept of multi-bifurcation steering is guiding the particles inside the safe zones and transferring the particles between the safe zones when the MNPs reach a bifurcation. Fig. 2 B illustrates the multi-bifurcation guidance strategy for a sample network.

This paper is organized as follows: section 2 presents the proposed model and algorithm; section 3 gives the simulation results and discusses them; and section 4 presents the conclusions.

2 Method

2 1 Modeling for particle steering

The size of nanoparticles can vary depending on the clinical application (the biological barrier that they were designed to cross). It also depends on the magnetic field applied. Further information regarding clinical use of MNPs and method for steering smaller MNPs can be found in [24, 25]. In order to utilize the discrete element method (DEM), the nanoparticles are assumed to be sufficiently large (> 500 nm) [26]. As the MNPs are bigger than 500nm, the Brownian motion which is more effective in smaller sized particles is excluded from the model [27]. Thus, Newtonian dynamics can be used for particle steering (Eq. 1).

$$m_i \frac{d\mathbf{v}_{pi}}{dt} = \mathbf{F}_{MF} + \mathbf{F}_{drag} + \mathbf{F}_m + \mathbf{F}_{etc} \tag{1}$$

where the subscript i indicates particle i, m_i is the particle mass, v_{pi} is the particle velocity, $\boldsymbol{F}_{MF}$ is the magnetic force, $\boldsymbol{F}_{drag}$ is the hydrodynamic drag force, $\boldsymbol{F}_m$ is the gravitational force (gravity and buoyancy), and $\boldsymbol{F}_{etc}$ includes un-modeled forces like electrostatic and adhesive forces, which are neglected due to their small contributions. The drag force on the particles is derived using Stokes' Law as:

$$\mathbf{F}_{drag} = -3\pi\eta d(\mathbf{v}_p - \mathbf{v}_f) \tag{2}$$

where v_p and v_f are the particle and fluid velocities, respectively, d is the particle diameter, and η is the fluid viscosity. The gravity and buoyancy force is described as follows:

$$\mathbf{F}_m = \frac{1}{6}\pi d^3(\rho_p - \rho_b)\mathbf{g} \tag{3}$$

where d is the particle diameter, $\mathbf{g}$ is the gravity constant, and ρ_p and ρ_b are the densities of the particle and blood, respectively. As buoyancy and gravity have opposite directions, the total force exerted on the particles is presented in Eq. 3 ($\boldsymbol{F_m}$). For all cases, the direction of $\boldsymbol{F_m}$ is along the -Z axis (X and Y are shown in Fig. 2 B, and Z is defined by the Right-hand Rule). $\boldsymbol{F}_{MF}$ is the steering force that is presented in the next subsection.

The MNPs are subjected to a magnetic force in the magnetic field, which is used as an actuation force to steer the MNPs and is defined as:

$$\mathbf{F}_{MF} = V\mu_1 M_{sat}\nabla\mathbf{H}_f \tag{4}$$

where M_{sat} is the magnetic polarization, $\nabla \boldsymbol{H}_f$ is the functionalized gradient of the magnetic intensity, the permeability in the medium is considered to be $\mu_1 = \mu_0$ (μ_0 is the permeability of the free space), and the aggregates are considered to be rod-shaped and their volume is represented as V. The aggregates have a diameter of d (individual particle's diameter) and height of h. The height of a rod-shaped aggregate is nd, where n is the number of nanoparticles in the aggregate. The aggregate has a volume of $V=\pi/4(nd^3)$; therefore, the diameter of an equivalent spherical particle for the simulation is described as:

$$d_{eq} = \sqrt[3]{3n}\, d \tag{5}$$

In the simulation, to illustrate the aggregation effects, the particles are considered to have equivalent diameter d_{eq}. The functionalized gradient field is defined as:

$$\nabla\mathbf{H}_f = SF(t)\nabla\mathbf{H} \tag{6}$$

where $\nabla \boldsymbol{H}$ is the gradient field and $SF(t)$ is the user-defined function, which consists of the following parts:

$$SF(t)\begin{cases} AFF(t) & t < t_{trS_1} & 1 \le AFF \le -\alpha \\ TFF(t) & t_{trS_1} \le t \le t_{trS_1} + T_E & TFF = -1 \\ SFF(t) & t_{trS_1} + T_E < t < \cdots & \alpha \le SFF \le -\alpha \\ \vdots & \vdots & \vdots \\ TFF(t) & t_{trS_n} \le t \le t_{trS_n} + T_E & TFF = 1 \\ SFF(t) & t_{trS_n} + T_E < t < \cdots & \alpha \le SFF \le -\alpha \\ \vdots & \vdots & \vdots \end{cases} \tag{7}$$

The t_{trS} is the starting time of the transport function (TFF), T_E is the duration of transport, and α is the asymmetry ratio. The SF (Fig. 2 A) is given mainly by the three functions in Eq. (7). The asymmetrical field function (AFF) is designed to capture and guide all particles to the first safe zone. The transporter field function (TFF) is designed

to transport all particles to the next Safe Zone. The sustainer field function (SFF) is designed to keep the particles within the safe zone and facilitate movement of the particles with the flow (all three functions are illustrated separately in Fig. 2 B). The minus sign means that the actuation is applied in the reverse direction (here it is the right coil).

Once the MNPs aggregate, they are subject to a stronger magnetic force, which causes them to move rapidly inside the vessel. To compensate for this high magnetic force and to keep the particles inside the safe zone, a field function with an asymmetrical magnitude is proposed (AFF). The asymmetry of the AFF is designed to impose more force in the direction of, and capture all particles inside, the safe zone. At the same time, α (the asymmetry ratio) is designed to prevent the particles from leaving the safe zone and to move them forward with the blood flow until the particles reach the second bifurcation (t_{trs1}, illustrated in Fig. 3).

Then, TFF is used to transfer the MNPs to the next safe zone; the TFF activates the EMA in the reverse direction and transports all of the particles to the second safe zone. The force is applied during the period T_E, which is the time needed for all particles to move into the next safe zone (illustrated in Fig. 3).

The SFF is used to keep the particles within the safe zone without sticking. The same sequence of TFF-SFF can be applied to steer the particles through the remaining bifurcations.

Fig. 3 illustrates the particle path with multi-bifurcation guidance. When there is no magnetic force (illustrated in grey), the minimum time for the MNPs to reach the first bifurcation is defined as T_L. With EMA guidance (illustrated in red), the minimum time needed to steer all of the particles to the safe zone is T_c. Incorporating the forces in Eq. 1, the trajectories of the particles can be determined.

2 3 Algorithm for guidance

The Flowchart in Fig. 4 was used to design and optimize the SF in COMSOL software (COMSOL, Palo Alto, CA, USA). Initially, a CAD model and the simulation constants were imported to the software using the information in Table 1. The algorithm has three distinct steps for SF design.

Initially, the minimum required time to guide all particles to the safe zone (T_c) must be determined using the simulation software. The time to guide particles to the safe zone is directly linked to the magnitude of the magnetic force (Eq. 4) and the magnetic force is a function of the gradient field (∇H). Therefore, if ∇H is chosen initially, the condition $T_L > T_c$ should be checked. If the condition is not satisfied, the gradient field should be increased gradually until all particles are in the safe zone. The maximum gradient field ($\nabla H = 2.23 \times 10^6$ (A/m^2)) is applied in the simulation based on the maximum gradient field applicable in our previously used experimental setup [17].

Although higher values for the gradient field can be achieved, we limit the parameter (maximum ∇H = 2.3 MA/m^2) to show a possible realistic implementation of the developed simulations.

The first step is to capture and move all of the MNPs inside the safe zone. The AFF consists of the following parameters: the asymmetry ratio α and the frequency with a 2-to-1 duty ratio (illustrated in Fig. 2). The 2-to-1 duty ratio in the AFF imposes more force towards the safe zone and captures all the particles. The frequency is considered sufficiently high to prevent the particles from leaving the safe zone (the simulation considers a constant frequency). The asymmetry ratio α is in the range $0 < \alpha \leq 1$ to facilitate movement of the particles inside the safe zone, and to prevent the particles from sticking and showing aggregation effects. The simulation determines the minimum time required for the particles to reach the second bifurcation (t_{trs}) when the AFF is applied (see t_{trs1} in Fig. 3). In real experiments, this time can be measured using the real-time MPI monitoring system introduced in [28]. Since the branches used in the simulation have similar geometries, t_{trs} is initially considered to be $2T_L$. Upon checking the particle trajectory, if the particles have not reached the second bifurcation, the operating time t_{trs} for AFF is increased until the condition is satisfied.

In the second step, T_E (the time required to execute TFF) is considered to be two times T_c to guide all the MNPs to the next safe zone, and the magnitude of *TFF* is considered to be 1. In the third step, to keep the particles inside the second safe zone and move them toward the desired outlet, a SFF of magnitude equal to α is used (a 1-to-1 duty ratio). This function is used to facilitate particle movements inside the safe zone. The third and fourth steps of the algorithm can be repeated for guidance through multiple bifurcations. To study the targeting performance, the algorithm was used for different values of asymmetry α and various blood velocities.

3. Results and discussion

We imported the multi-channel model into COMSOL and used the particle-tracking module to study the proposed EMA actuation scheme for multi-channel guidance.

3. 1 Simulation and results

A multi-bifurcation vessel (as shown in Fig. 2 B with 45˚ angle from vessel direction for all branches) with one inlet and four outlets (all with a diameter of 1 mm) and a length of 5 mm (for all branches) was modelled. A steady state blood flow (with 1:1 distribution in the bifurcations) was simulated inside the channels and the velocity profile for the multi-bifurcation vessel was calculated using the computational fluid dynamics CFD module of COMSOL. The drag force was also considered in the simulation. The 3D model was generated and automatically meshed.

Experimental studies in [15] indicate that the majority of MNPs in a magnetic field form rod-shaped aggregates. To match the simulation with the experimental data, the average aggregate was considered to be 100 μm high (the simulation constants are presented in Table 1). The particles were assumed to be spherical MNPs with a diameter of d_{eq} and density of 2.25 g/cm3. The particle simulation motions based on the EMA actuation match the guidance time T_c for the Safe Zone reported in experimental studies [15] (illustrated in Fig. 4A).

Three bifurcations were used in this simulation and 1,000 particles were released at the inlet; however, the same approach can be extended to more bifurcations. The simulation results in Fig. 5B, show that the particles are steered magnetically using SF(t) to reach the targeted outlet.

Table 2 summarizes the simulation results for the time needed to reach the first bifurcation. These indicate that MNPs reach the bifurcation very quickly with a high blood velocity and the proposed design loses its feasibility. The trend is shown in Fig. 5C. Fig. 5C-3 illustrates that for V_f = 10 mm/s, some particles exit the safe zone and 100% guidance is not achievable.

The time needed for all the particles to enter the safe zone depends on the gradient field (∇ H). Fig. 5A shows that T_c in this simulation is in agreement with the results published in [17]. Fig. 5D shows that the higher gradient field quickly captures the particles in the simulation and makes particle steering more feasible.

3. 2 Discussion

The number of MNPs reaching the desired outlet is calculated by the software and is considered as an indicator of success. Fig. 6 presents the targeting results for different magnitudes of α and different blood velocities. The blood velocity is varied between 0.5 and 100 mm/s (the blood velocity in capillaries varies between 0.5 and 1 mm/s [29]) and the asymmetry ratio α is varied between 0.16 and 1. Also, it shows that in the absence of a magnetic force, only a small portion of the particles (first column in Fig. 6 for all velocity conditions) reaches the desired outlet, which is located in the far branch of the multi-bifurcation network (Fig. 5B). This indicates that for lower velocities, the targeting performance could reach 100%. Although 100% targeting cannot be achieved for a velocity equal to 10 mm/s, a maximum 98.5% targeting performance can be achieved. Fig. 6 indicates that the targeting performance varies slightly when α is varied between 0.16 and 1. It also shows that with a high blood velocity, the targeting performance is reduced. This occurs because T_L is very small and all particles cannot enter the safe zone (the first condition $T_L > T_c$ is not satisfied); and there are always some particles in the incorrect outlet (illustrated in Fig. 5C-1). Despite this decrease in targeting performance, for velocities as high as 25 mm/s, a targeting rate of 57% can be achieved, which indicates an acceptable performance even at a high blood velocity.

The limitation of the scheme is also shown in Fig. 6, where under very high flow velocity (100 mm/s) conditions, the guidance strategy loses performance and becomes ineffective. In conclusion, Fig. 6 indicates that the success in MNPs steering depends on flow velocity. For velocities up to 5 mm/s, 100% of MNPs exit the first branch and can be guided to the desired outlet. However, if the low flow velocity cannot be achieved, the success rate of MNPs steering will decrease.

The strategy for swarm nanoparticles steering under fluid flow is discussed and simulated in the current study. The results have encouraged us to perform further experimental studies in the future. The proposed scheme has two possible applications: 1) it can be used for in vitro lab on chip applications to deliver cargoes using MNPs or swarm of microrobots in a complex multi bifurcation environment, 2) it can be used as a magnetic navigation system for in vivo drug delivery using our recently developed MPI which has a millimetre scale, fast response (<0.5 s frame update rate), and 60 mm × 60 mm region of interest [15, 30-32]. Although the region of interest is too small for human scale application, it can be used for in vivo animal tests. The region of 60 mm × 60 mm is chosen based on previously developed experimental set-up for MPI-based magnetic nanoparticle monitoring and steering [32]. MPI has already been tested in vivo on small animals [33] and in the most recent works, its potential to be scaled up for applications in the human brain was explored [34].

Despite the immediate potential for in vitro applications, further system developments of MPI in terms of region of interest, image quality, and simultaneous monitoring and actuation functions are required for use in clinical applications. Furthermore, for in vivo clinical experiments, it is necessary to control the blood flow using techniques like temporary embolization [23]. On the other hand, the scheme presented here can be used with pre-clinical systems such as X-ray and MRI based navigation [14, 35]. To sum up, the proposed scheme can be successfully used in the future for in vivo and in vitro applications.

4 Conclusion

The recently developed MPI system has made feasible the implementation of a steering scheme in multi-bifurcation blood vessels. This paper proposes an electromagnetic-based steering scheme for guiding swarms of MNPs inside a multi-bifurcation network. The proposed magnetic steering scheme can successfully guide nanoparticles between the safe zones and steer them toward the desired outlet. With low blood velocities, a targeting performance of 100% is achieved. With higher blood velocities, the targeting performance is reduced. However, even for a blood velocity of 25 mm/s, a targeting performance of 57% is achieved, which shows that the proposed scheme has a high targeting performance for a broad range of blood velocities. Future work should

include a user in the loop control strategy, as most targeted drug delivery systems are semi-automatic and a human controls the MDT to ensure safety.

Acknowledgment

This research was funded by the National Research Foundation (NRF) of Korea (2017R1A2B4011704 & 2019M3C1B8090798) and Korea Evaluation Institute of Industrial Technology (KEIT) grant (No. 20003822).

TABLE 1

The simulation constants

Symbol	Parameter	
ρ_p	Particle density	2.25 g/cm^3
d	Particle diameter	800 nm
ρ_b	Blood density	1.05 g/cm^3
η	Blood viscosity	0.004 Pa.s
T	Blood temperature	293.15 K
L	Average aggregate length	100 μm
n	Average number of particles	125
T_E	Time for guiding MNPs to Safe Zone	$T_E = 2T_c$
d_{eq}	Equivalent diameter	5.6 μm
∇H	Gradient field	2.23 (MA/m^2)
M_{sat}	Magnetic polarization	58 (emu/g)
Fr_{AFF}	Frequency of AFF	*1.23 Hz*
Fr_{SFF}	Frequency of SFF	*1.85 Hz*

TABLE 2

The time needed by MNPs to reach the first bifurcation (T_L) for different flow velocities.

Symbol			
T_L	2.61 s	0.52 s	0.26 s
v_f	1 mm/s	5 mm/s	10 mm/s

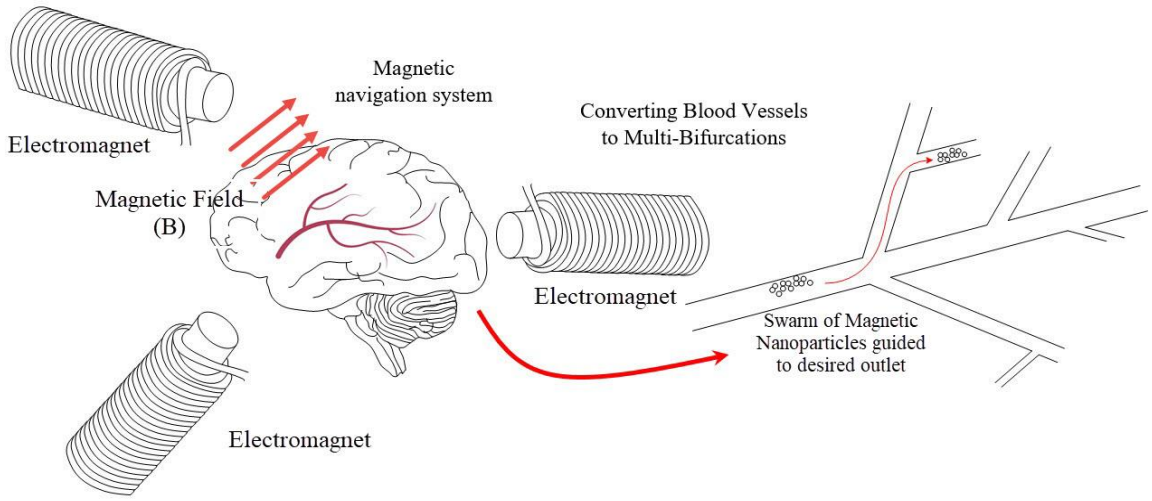

Fig. 1 Multiple bifurcations assumption for steering magnetic nanoparticles (MNPs)

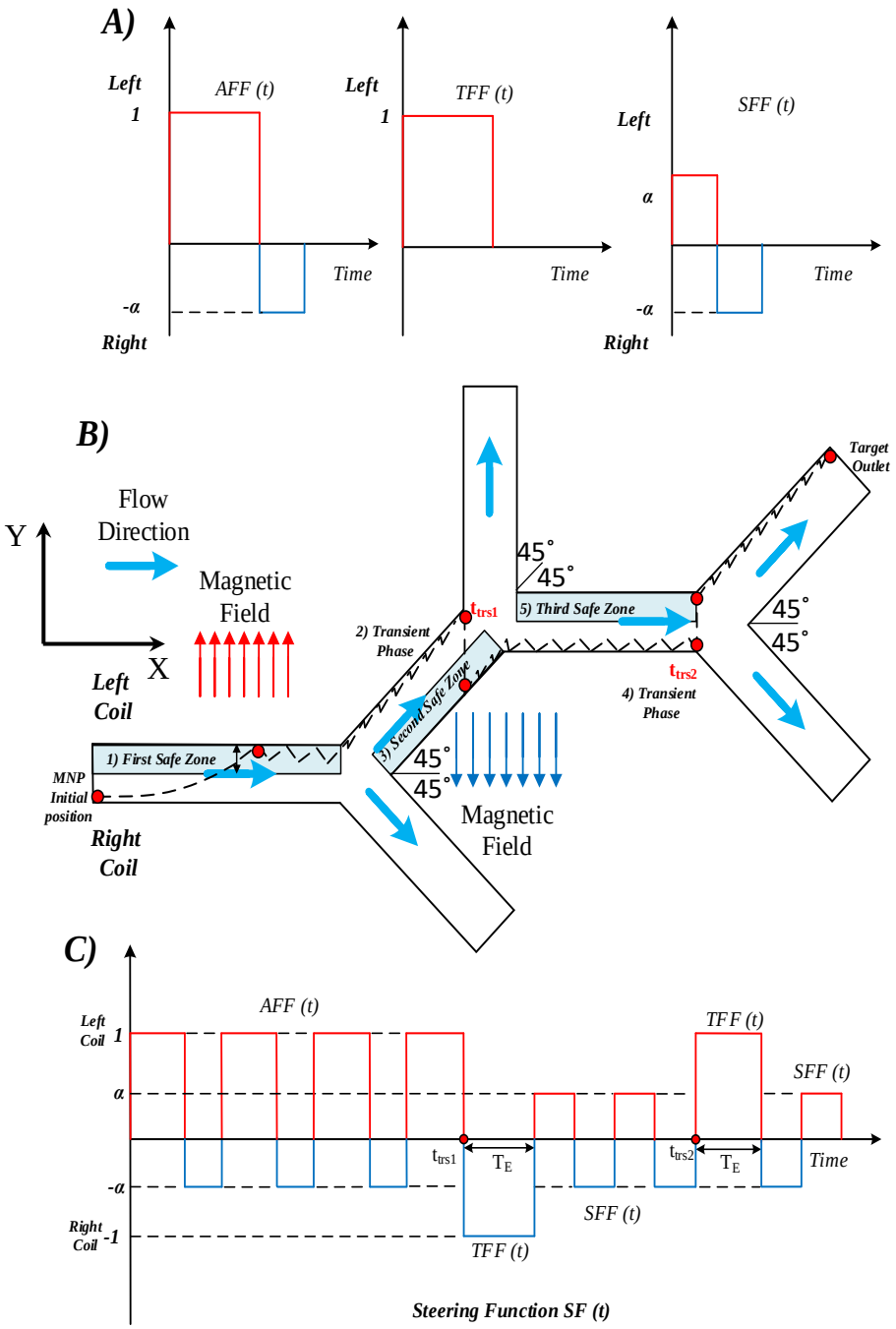

Fig. 2 A) The asymmetrical field function (AFF), transporter field function (TFF), and sustainer field function (SFF). B) The multi-bifurcation channel with one inlet and four outlets, C) steering function *SF*(*t*).

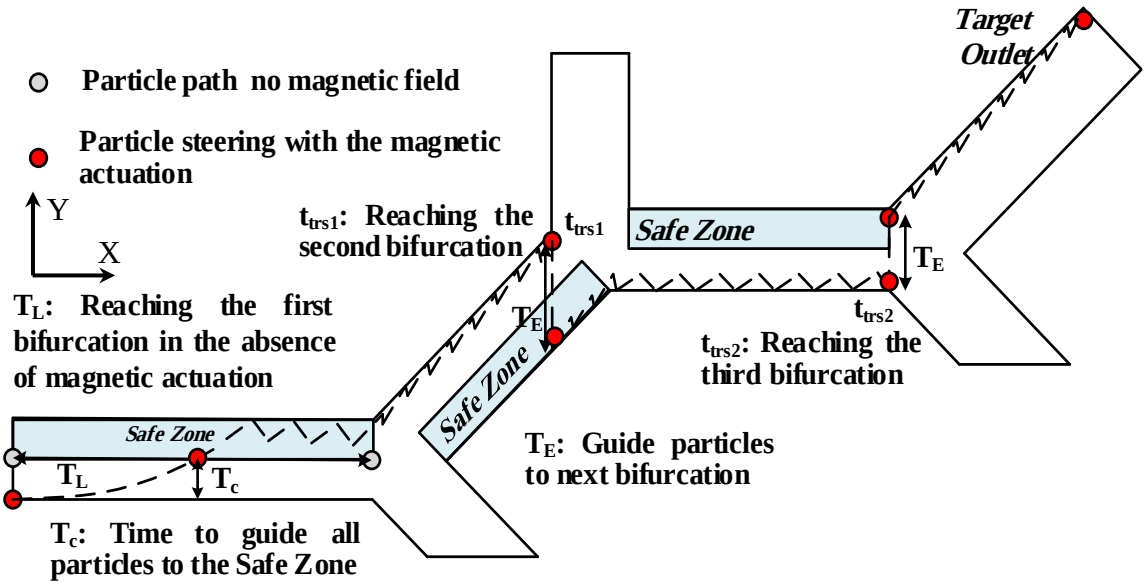

Fig. 3. The particle path and electromagnetic actuator (EMA) acuation for guidence.

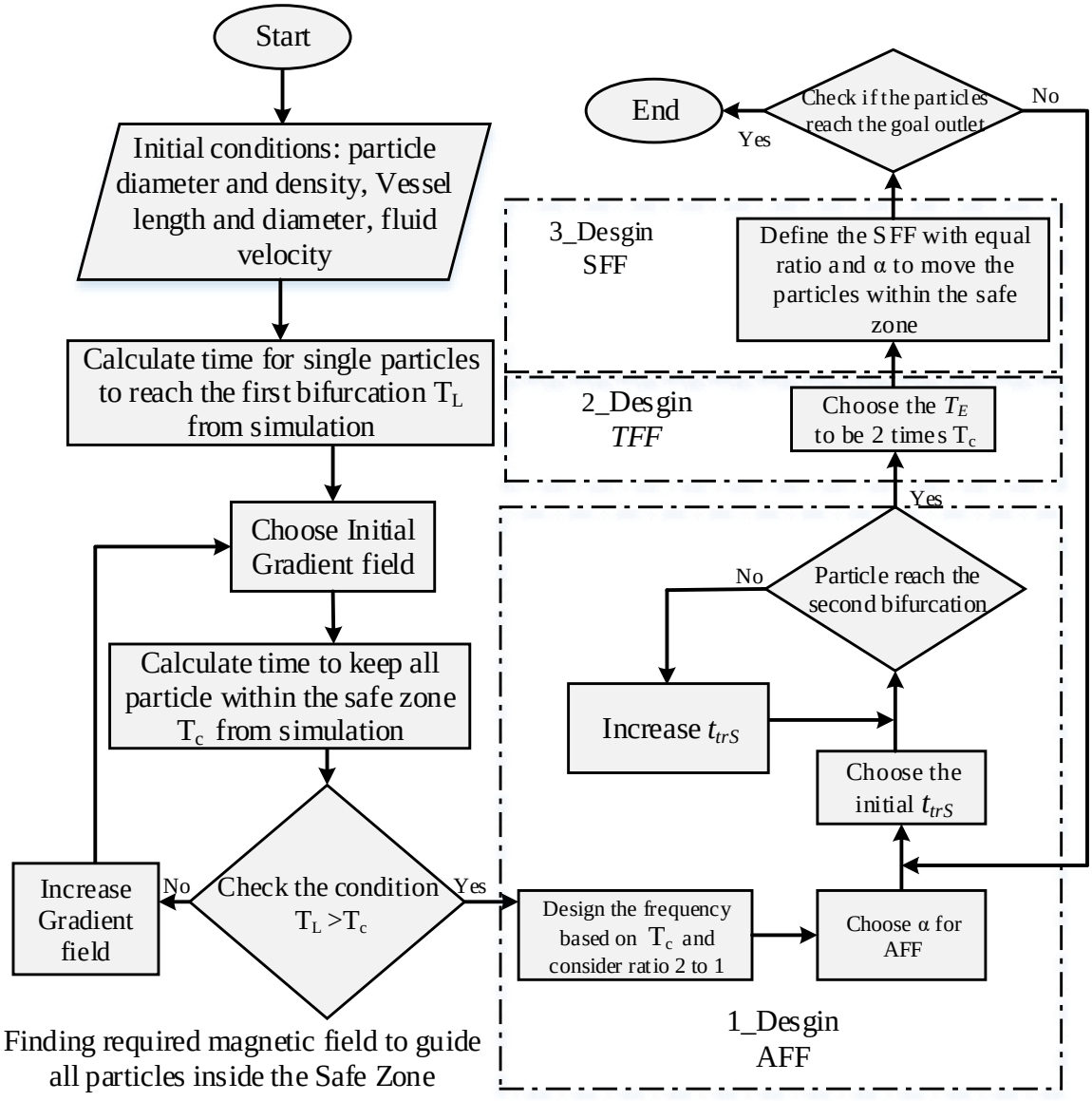

Fig. 4. Simulation flowchart used to design the SF for MNP guidance in a multi-bifurcation vessel.

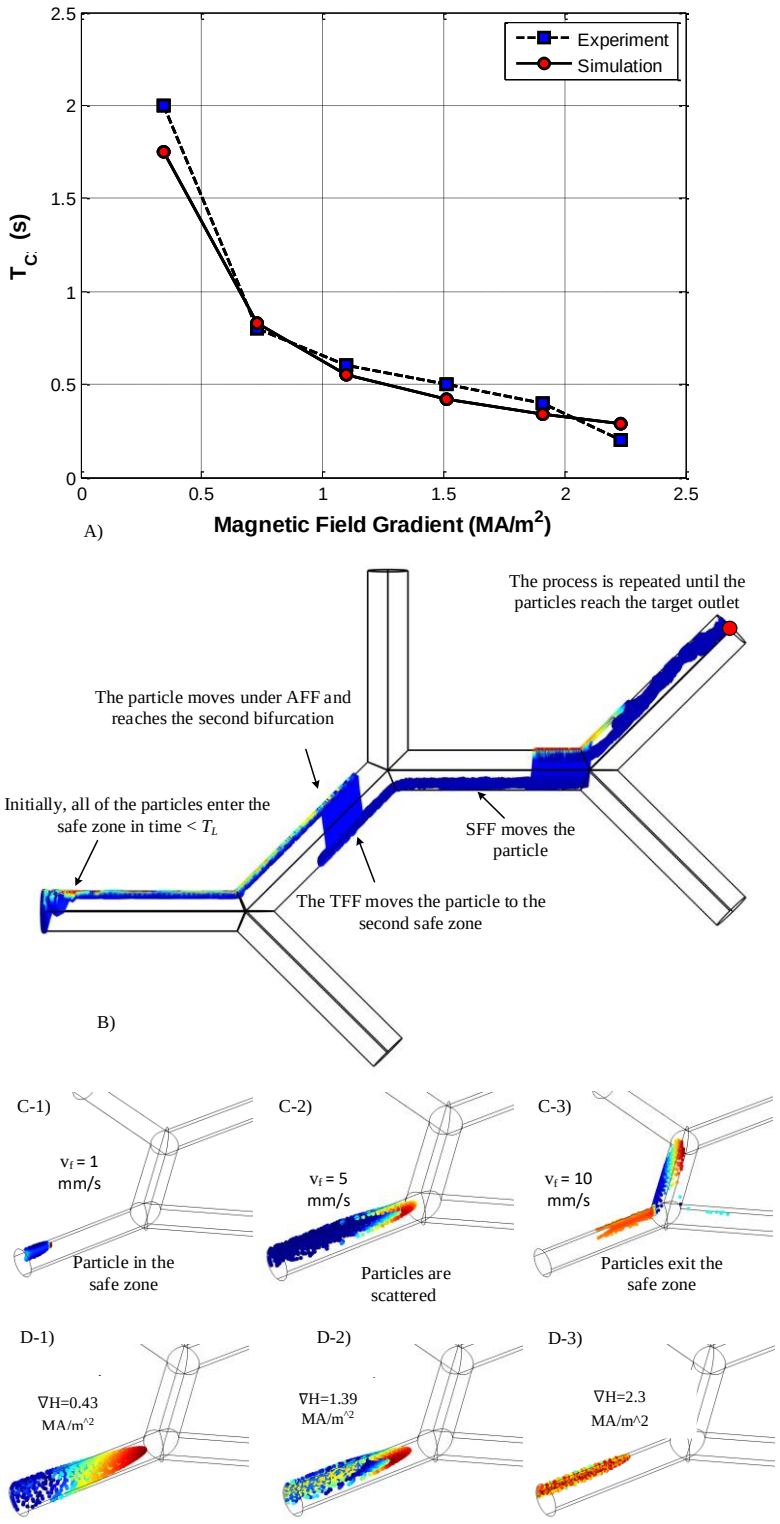

Fig. 5. A) Comparing the experimental results [9] with the simulation. B) Particle tracking under the designed SF(t) (the particle path from inlet to outlet is illusturated) can guide the particles to the desired outlet (V_f = 0.5 mm/s and ∇H = 2.3 MA/m^2). C) Particle tracking simulation to show the effects of different velocities. D) Particle tracking simulation to show the effects of different magnetic fields (V_f = 0.5 mm/s, simulaton time T_s = 0.5 s).

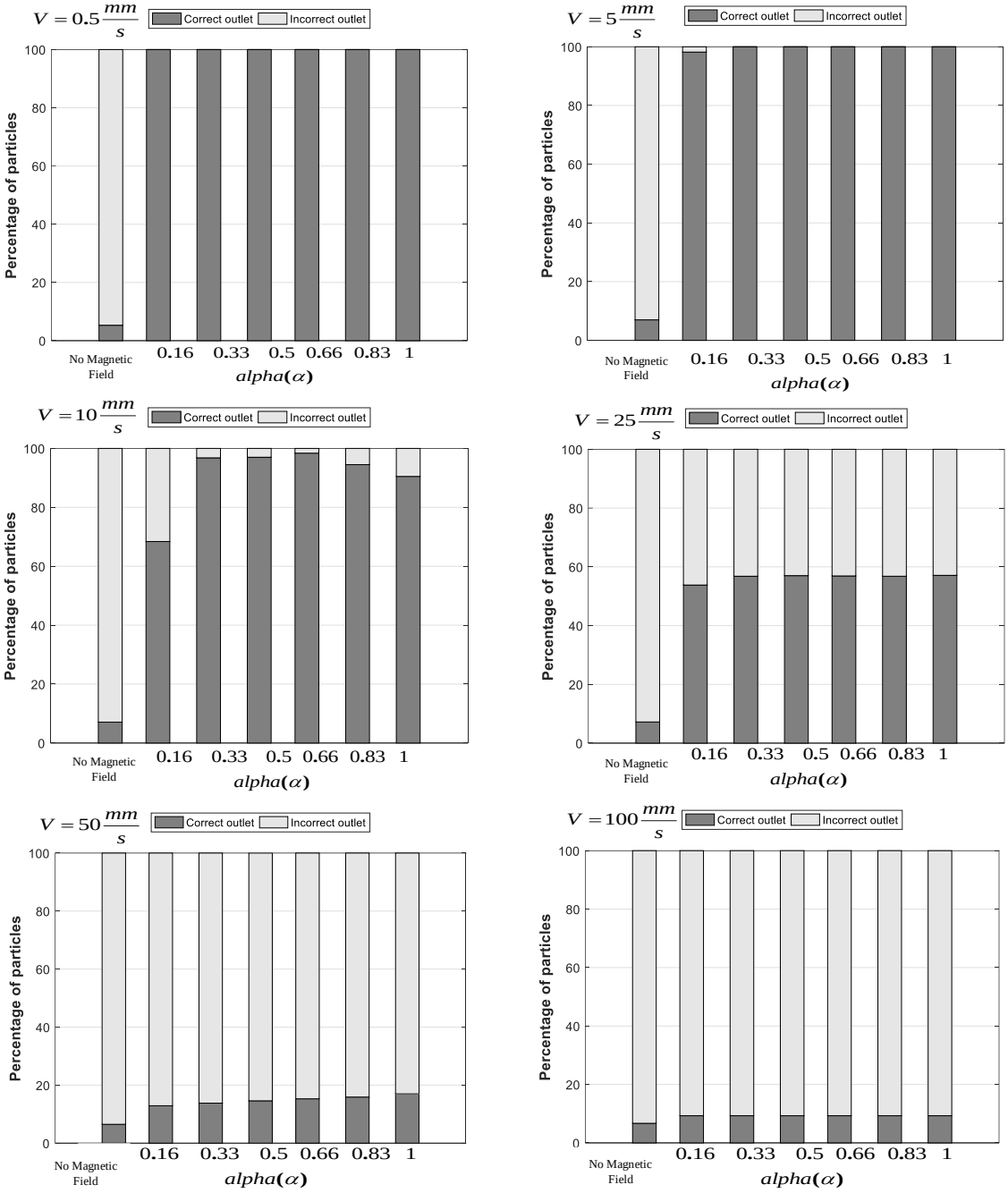

Fig. 6. Distribution of particles reaching the correct and incorrect outlets under different velocities and SF(t) conditions.

References

[1] S. Doostie, A. K. Hoshiar, M. Nazarahari, S. Lee, and H. Choi, "Optimal path planning of multiple nanoparticles in continuous environment using a novel Adaptive Genetic Algorithm," *Precision Engineering*, vol. 53, pp. 65-78, 2018.

[2] A. K. Hoshiar and H. RaeisiFard, "A Simulation Algorithm for Path Planning of Biological Nanoparticles Displacement on a Rough Path," *Journal of Nanoscience and Nanotechnology*, vol. 17, no. 8, pp. 5578-5581, 2017.

[3] A. H. Korayem, A. K. Hoshiar, and M. H. Korayem, "Modeling and simulation of critical forces in the manipulation of cylindrical nanoparticles," *International journal of Advanced Manufacturing Technology*, vol. 79, 2015.

[4] B. J. Nelson, I. K. Kaliakatsos, and J. J. Abbott, "Microrobots for minimally invasive medicine," (in eng), *Annu. Rev. Biomed. Eng.*, vol. 12, pp. 55-85, Aug 15 2010.

[5] P. Kheirkhah *et al.*, "Magnetic Drug Targeting: A Novel Treatment for Intramedullary Spinal Cord Tumors," *Sci. Rep.*, vol. 8, no. 1, p. 11417, 2018/07/30 2018.

[6] K. T. Al-Jamal *et al.*, "Magnetic Drug Targeting: Preclinical in Vivo Studies, Mathematical Modeling, and Extrapolation to Humans," *Nano Lett.*, vol. 16, no. 9, pp. 5652-5660, 2016/09/14 2016.

[7] X. Ding *et al.*, "Hydrazone-Bearing PMMA-Functionalized Magnetic Nanocubes as pH-Responsive Drug Carriers for Remotely Targeted Cancer Therapy in Vitro and in Vivo," *ACS Applied Materials & Interfaces*, vol. 6, no. 10, pp. 7395-7407, 2014/05/28 2014.

[8] H. Choi *et al.*, "EMA system with gradient and uniform saddle coils for 3D locomotion of microrobot," *Sensors and Actuators A: Physical*, vol. 163, no. 1, pp. 410-417, 2010.

[9] S. Jeong, H. Choi, J. Choi, C. Yu, J.-o. Park, and S. Park, "Novel electromagnetic actuation (EMA) method for 3-dimensional locomotion of intravascular microrobot," *Sensors and Actuators A: Physical*, vol. 157, no. 1, pp. 118-125, 2010.

[10] M. P. Kummer, J. J. Abbott, B. E. Kratochvil, R. Borer, A. Sengul, and B. J. Nelson, "OctoMag: An Electromagnetic System for 5-DOF Wireless Micromanipulation," *IEEE Transactions on Robotics*, vol. 26, no. 6, pp. 1006-1017, 2010.

[11] J. Yu, B. Wang, X. Du, Q. Wang, and L. Zhang, "Ultra-extensible ribbon-like magnetic microswarm," *Nature communications*, vol. 9, no. 1, p. 3260, 2018.

[12] B. Wang *et al.*, "Reconfigurable Swarms of Ferromagnetic Colloids for Enhanced Local Hyperthermia," *Adv. Funct. Mater.*, 2018.

[13] M. Latulippe and S. Martel, "A Progressive Multidimensional Particle Swarm Optimizer for magnetic core placement in Dipole Field Navigation," in *2016 IEEE/RSJ International Conference on Intelligent Robots and Systems (IROS)*, 2016, pp. 2314-2320.

[14] M. Vonthron, V. Lalande, G. Bringout, C. Tremblay, and S. Martel, "A MRI-based integrated platform for the navigation of micro-devices and microrobots," in *2011 IEEE/RSJ International Conference on Intelligent Robots and Systems*, 2011, pp. 1285-1290.

[15] T.-A. Le, X. Zhang, A. K. Hoshiar, and J. Yoon, "Real-Time Two-Dimensional Magnetic Particle Imaging for Electromagnetic Navigation in Targeted Drug Delivery," *Sensors*, vol. 17, no. 9, p. 2050, 2017.

[16] A. K. Hoshiar, T.-A. Le, F. U. Amin, M. O. Kim, and J. Yoon, "Functionalized electromagnetic actuation method for aggregated nanoparticles steering," in *Engineering in Medicine and Biology Society (EMBC), 2017 39th Annual International Conference of the IEEE*, 2017: IEEE, pp. 885-888.

[17] A. K. Hoshiar, T.-A. Le, F. U. Amin, M. O. Kim, and J. Yoon, "Studies of aggregated nanoparticles steering during magnetic-guided drug delivery in the blood vessels," *J. Magn. Magn. Mater.*, vol. 427, pp. 181-187, 2017.

[18] T. A. Le, A. K. Hoshiar, T. D. Do, and J. Yoon, "A modified functionalized magnetic Field for nanoparticle guidance in magnetic drug targeting," in *2016 13th International Conference on Ubiquitous Robots and Ambient Intelligence (URAI)*, 2016, pp. 493-496.

[19] F. U. Amin *et al.*, "Osmotin-loaded magnetic nanoparticles with electromagnetic guidance for the treatment of Alzheimer's disease," *Nanoscale,* 10.1039/C7NR00772H vol. 9, no. 30, pp. 10619-10632, 2017.

[20] A. K. Hoshiar, T.-A. Le, F. U. Amin, M. O. Kim, and J. Yoon, "A Novel Magnetic Actuation Scheme to Disaggregate Nanoparticles and Enhance Passage across the Blood–Brain Barrier," *Nanomaterials,* vol. 8, no. 1, p. 3, 2018.

[21] F. Michaud *et al.*, "Selective embolization with magnetized microbeads using magnetic resonance navigation in a controlled-flow liver model," *Med. Phys.*, vol. 46, no. 2, pp. 789-799, 2019.

[22] N. Li *et al.*, "Magnetic Resonance Navigation for Targeted Embolization in a Two-Level Bifurcation Phantom," *Ann. Biomed. Eng.*, vol. 47, no. 12, pp. 2402-2415, 2019.

[23] S. Martel, "Magnetic Navigation Control of Microagents in the Vascular Network: Challenges and Strategies for Endovascular Magnetic Navigation Control of Microscale Drug Delivery Carriers," *IEEE Control Systems,* vol. 33, no. 6, pp. 119-134, 2013.

[24] J. S. Weinstein *et al.*, "Superparamagnetic iron oxide nanoparticles: diagnostic magnetic resonance imaging and potential therapeutic applications in neurooncology and central nervous system inflammatory pathologies, a review," *J. Cereb. Blood Flow Metab.*, vol. 30, no. 1, pp. 15-35, 2010.

[25] Z. Nosrati *et al.*, "Development of a coflowing device for the size-controlled preparation of magnetic-polymeric microspheres as embolization agents in magnetic resonance navigation technology," *ACS Biomaterials Science & Engineering,* vol. 4, no. 3, pp. 1092-1102, 2018.

[26] P. Vartholomeos, M. Fruchard, A. Ferreira, and C. Mavroidis, "MRI-guided nanorobotic systems for therapeutic and diagnostic applications," *Annu. Rev. Biomed. Eng.*, vol. 13, pp. 157-184, 2011.

[27] P. I. Dolez, *Nanoengineering: global approaches to health and safety issues*. Elsevier, 2015.

[28] X. Zhang, T.-A. Le, and J. Yoon, "Development of a real time imaging-based guidance system of magnetic nanoparticles for targeted drug delivery," *J. Magn. Magn. Mater.*, vol. 427, pp. 345-351, 2017.

[29] J. B. Mathieu and S. Martel, "Steering of aggregating magnetic microparticles using propulsion gradients coils in an MRI Scanner," *Magn. Reson. Med.*, vol. 63, no. 5, pp. 1336-45, May 2010.

[30] T. Le, X. Zhang, A. K. Hoshiar, and J. Yoon, "An electromagnetic navigation system with real-time 2D magnetic particle imaging for targeted drug delivery," in *2017 IEEE/RSJ International Conference on Intelligent Robots and Systems (IROS)*, 2017, pp. 1895-1900.

[31] A. K. Hoshiar, T.-A. Le, F. U. Amin, X. Zhang, M. O. Kim, and J. Yoon, "19 Noninvasive Guidance Scheme of Magnetic Nanoparticles for Drug Delivery in Alzheimer's Disease," *Clinical Applications of Magnetic Nanoparticles,* p. 343, 2018.

[32] X. Zhang, T. A. Le, A. K. Hoshiar, and J. Yoon, "A Soft Magnetic Core Can Enhance Navigation Performance of Magnetic Nanoparticles in Targeted Drug Delivery," *IEEE/ASME Transactions on Mechatronics,* pp. 1-1, 2018.

[33] B. Zheng *et al.*, "Magnetic Particle Imaging tracks the long-term fate of in vivo neural cell implants with high image contrast," *Sci. Rep.*, vol. 5, no. 1, p. 14055, 2015/09/11 2015.

[34] M. Graeser *et al.*, "Human-sized magnetic particle imaging for brain applications," *Nature Communications,* vol. 10, no. 1, p. 1936, 2019/04/26 2019.

[35] A. J. Petruska, J. Edelmann, and B. J. Nelson, "Model-Based Calibration for Magnetic Manipulation," *IEEE Trans. Magn.*, 2017.